Pure Appl. Chem., Vol. 76, Nos. 7–8, pp. 1537–1545, 2004.

Structure–function investigation of a deoxyribozyme with dual chelatase and peroxidase activities*

Hyun-Wu Lee, Daniel J.-F. Chinnapen, and Dipankar Sen‡

Department of Molecular Biology and Biochemistry, Simon Fraser University, Burnaby, British Columbia V5A 1 S6, Canada

Abstract: PS2.M, an 18-nucleotide DNA molecule, has been shown to be a dual enzyme for porphyrin metallation and, when complexed with hemin, for peroxidation. To date, detailed information has not been available on either the actively folded structure of PS2.M or on the contribution of specific nucleotides within it toward the peroxidase activity. Here, we report a variety of experiments that probe the structure and function of PS2.M as well as of a number of point mutants of PS2.M. Based on these experiments, a structural model for the folding of PS2.M and the location of a functionally relevant hemin-binding site are proposed. A key finding is that PS2.M, originally obtained by in vitro selection from a random-sequence DNA library, is uniquely suited for its catalysis of peroxidation; all point mutants examined showed significantly poorer catalytic activity than PS2.M itself.

INTRODUCTION

The discovery of catalytic RNA molecules (ribozymes) in nature [1,2] gave rise to the hypothesis of an "RNA World" for the origin of life [3], according to which extant DNA, RNA, and protein-based life forms were preceded by RNA molecules capable of self-replication as well as the chemical catalysis of a variety of metabolic reactions. The RNA World hypothesis has stimulated interest into investigating the catalytic repertoire available to RNA and RNA-like polymers, such as DNA. The search for such new RNA and DNA catalysts has been facilitated, in turn, by the development of in vitro selection (SELEX) methodologies [4,5], whereby RNA and DNA molecules possessing binding and/or catalytic properties of interest are iteratively selected out from large, random-sequence RNA/DNA libraries.

Both direct and indirect SELEX approaches have been used for the selection of novel ribozymes and deoxyribozymes (DNAzymes) (reviewed in ref. [6]). In the former, DNA and RNA molecules are selected directly for possessing a catalytic property, bypassing selection for any binding property to a potential substrate or transition-state analog. In the latter approach, binding DNA or RNA molecules ("aptamers") are sought for the specific and strong recognition and binding of stable transition-state analogs (TSAs) for the relevant reactions, with the expectation that such aptamers would prove catalytic for the reaction in question. Direct selections to date have yielded the majority of the novel RNA and DNA enzymes reported, whereas the TSA approach has yielded DNA and RNA enzymes for porphyrin metallation, which were selected on the basis of specific binding to a transition-state analog for the reaction, *N*-methylmesoporphyrin (NMM) [7].

*Lecture presented at the symposium "Chemistry of nucleic acids", as part of the 39th IUPAC Congress and 86th Conference of the Canadian Society for Chemistry: Chemistry at the Interfaces, Ottawa, Canada, 10–15 August 2003. Other Congress presentations are published in this issue, pp. 1295–1603.

‡Corresponding author

PS2.M was an 18-nucleotide deoxyribozyme that catalyzed porphyrin metallation [8–10]. The metalloporphyrin, hemin [iron(III)-protoporphyrin IX], a strong competitive inhibitor for the metallation reaction [9,11,12] was found to bind the folded PS2.M with a strong affinity (27 ± 2 nM). Curiously, the PS2.M-hemin complex also showed a DNA-enhanced peroxidative activity such that the $v_{cat}/v_{backgrd}$ ratio measured under optimized solution conditions was >250 ($v_{backgrd}$ refers to the peroxidative activity of disaggregated hemin in the presence of a control DNA oligomer) [11–14]. PS2.M was guanine-rich and required potassium ions to fold to its active conformation, consistent with its folding to form a guanine-quadruplex higher-order structure. Interestingly, the RNA version of PS2.M, rPS2.M, was also found to be a significant peroxidase when complexed with hemin [12].

Although PS2.M was only 18 deoxynucleotides long, the details of its folded and catalytically active structure have not been adequately elucidated to date. In this paper, we report a systematic mutational analysis of PS2.M, to understand its folding as well as obtain information on the features of its folded structure that contribute to hemin-binding and to the peroxidative activity. As described above, earlier experiments had established that PS2.M folded to form a guanine quadruplex. Here, we report the results of four categories of experiments on PS2.M and on a series of PS2.M point mutants. These include methylation protection analysis (both in the presence and in the absence of bound hemin); relative gel mobility of the folded DNAzymes in native gels; melting behavior of the folded DNAzymes in the presence of hemin; and, peroxidase activity of the DNAzymes complexed with hemin.

MATERIALS AND METHODS

Oligonucleotides

Oligonucleotides were synthesized at the University of Calgary Core DNA services. The sequence for the "wild-type" peroxidase deoxyribozyme PS2.M was 5′-GTG GGT AGG GCG GGT TGG-3′. Point mutations were then made in this sequence, to generate the following mutant oligonucleotides:

G12I: 5'-GTG GGT AGG GC**T** GGT TGG; **G12A**: 5'-GTG GGT AGG GC**A** GGT TGG

G17A: 5'-GTG GGT AGG GCG GGT T**A**G; **G18A**: 5'-GTG GGT AGG GCG GGT TG**A**

G5I: 5'-GTG G**I**T AGG GCG GGT TGG; **G5A**: 5'-GTG G**A**T AGG GCG GGT TGG

G10I: 5'-GTG GGT AGG **I**CG GGT TGG; **G10A**: 5'-GTG GGT AGG **A**CG GGT TGG

G1A: 5'-**A**TG GGT AGG GCG GGT TGG

Where required, 5′ end-labeling of oligonucleotides with ^{32}P was carried out using standard kinasing procedures.

Methylation protection assays

DNA oligonucleotides used for methylation protection experiments were pretreated with hot piperidine and were gel-purified, in order to obtain lower levels of background cleavage. For each sample, 1 μl of a very low concentration of ^{32}P-labeled PS2.M was supplemented with 1 μl of 10 μM unlabeled PS2.M. The solution was made up to 5 μl by addition of 10 mM Tris, pH. 8.0, 0.1 mM EDTA (TE buffer), and the DNA heat-denatured and cooled in a screw-capped tube. Five μl of potassium buffer (20 mM Tris-Cl, 40 mM KCl, and 1 % DMSO) were now added, and the DNA was allowed to fold at room temperature for 20 min (for the negative control, G-ladder, and T-ladder samples, ddH_2O was added instead of potassium buffer). For the hemin complexes, 1 μl from a 100 μM hemin stock (in dimethylsulfoxide)

was now added to the folded DNA, and the sample further was incubated at 22 °C for 20 min to allow the hemin to bind.

To 10 μl of folded DNA or DNA-hemin complex, 2 μl of a freshly prepared 1.2 % DMS solution was added, mixed, and incubated at 22 °C for 30 min. Following the incubation, 1 μg of glycogen was added, and the sample ethanol precipitated. The air-dried pellet was dissolved in 90 μl ddH_2O, to which 10 μl of piperidine was added. This solution was now heated at 90 °C for 30 min, and the piperidine and water were removed by successive rounds of lyophilization.

T-ladders

To a 5-μl sample of the DNA, 5 μl of a freshly prepared 10 mM $KMnO_4$ stock was added, and the sample was incubated for 5 min. The sample was then quenched with 4 μl of $KMnO_4$ stop solution (50 % allyl alcohol and 250 mM EDTA) and ethanol precipitated as above.

Native gel mobility analysis

10 μM PS2.M and mutant oligonucleotides, either complexed or uncomplexed to hemin (10 μM hemin), in potassium buffer (above) were loaded into a 15 % native polyacrylamide gel, run in 50 mM Tris borate running buffer supplemented with 5 mM KCl. Gels were run at 22 °C, and gel bands were quantitated using Molecular Dynamics ImageQuant software.

Kinetic measurements of peroxidase reactions

DNA oligonucleotides, at concentration of 0.1 μM, were either complexed or not complexed with 0.1 μM hemin (final) in 20 KH buffer (20 mM KCl, 50 mM HEPES, 0.05 % Trition X-100, 1 % DMSO, 0.2 M NaCl). The oxidation of an added ABTS [2,2′-azinobis(3-ethylbenzothiozoline)-6-sulfonic acid] substrate (5 mM) was initiated by injection of H_2O_2 (600 μM final), and was carried out as described in refs. [8,9]. Rates of ABTS oxidation were measured by monitoring the appearance of the ABTS radical cation with absorption at 414 nm in a Cary-3E UV-Vis Spectrophotometer.

Thermal denaturation analysis

Oligonucleotides complexed with hemin, at 2 μM concentrations each, were studied for their thermal melting behavior in 40 KH buffer (40 mM KCl, 50 mM HEPES, pH 7.0) at 295 nm, using a Cary-3E UV-Vis Spectrophotometer. The temperature range examined was 20–90 °C, and the rate of temperature change was set at 0.5 °C/min.

RESULTS AND DISCUSSION

Model for the folded structure of PS2.M

Figure 1 shows the methylation protection data on PS2.M folded in the presence of 20 mM KCl, both in the presence and absence of hemin. PS2.M DNA and hemin concentrations were each at 10 μM; given the measured association constant of ~30 nM [11,12], we would expect >95 % of the DNA to be present in the hemin-bound complex. Earlier experiments had indicated a superior peroxidase activity of PS2.M-hemin in MES buffer than in Tris (unpublished data). Methylation protection experiments were therefore carried out separately in either buffer, to investigate if any structural difference could be detected between the two cases. Figure 1 shows that in both buffers, PS2.M folded in the absence of hemin gave a unique methylation protection pattern, in which G3, G4, G8, G9, G13, G16, and G17 were substantially protected with respect to the G-ladder (lane 'GL'), whereas G5, G10, and G12 were

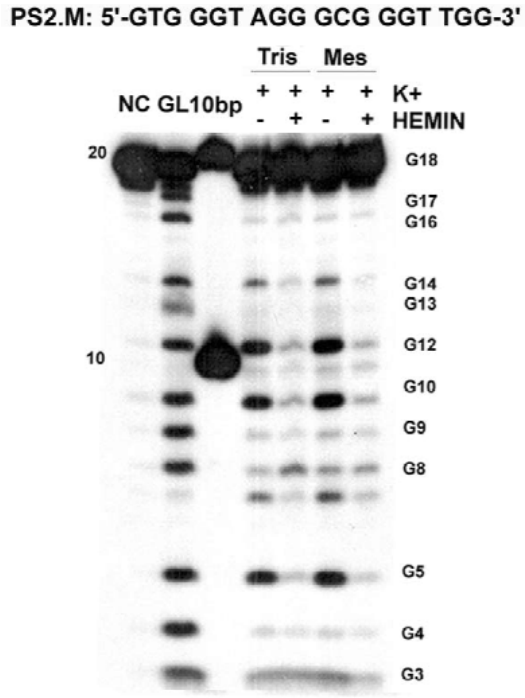

Fig. 1 Sequencing gel showing methylation protection data on PS2.M folded in the presence of 20 mM KCl, and either bound or not bound to hemin. The 'NC' lane shows PS2.M treated with dimethyl sulfate, but not piperidine. 'GL' shows a guanine ladder corresponding to PS2.M. '10 bp' shows a 10 b.p. ladder.

strongly reactive (G1 was difficult to monitor owing to its fast mobility in such a gel assay). On the basis of this protection pattern, two similar but topologically distinct folded models for PS2.M could be postulated (Fig. 2), both of which featured two guanine quartets and slightly different loop topologies. Interestingly, upon binding hemin the entire complement of guanines in PS2.M appeared to be substantially methylation-protected (Fig. 1, lanes 5 and 7). This suggested either a dramatic change in the quadruplex structure of folded PS2.M (forming, conceivably, three guanine quartets from the 12 available guanines) or else a potential involvement of the loop guanines (G5, G10, G12, and, possibly, G1) in interactions with the bound hemin(s). To test that the two-quartet quadruplex model of folded PS2.M (in the absence of bound hemin) was indeed correct, and also to investigate potential roles of individual loop guanines in interacting with bound hemin and thus with the catalysis of peroxidation, a number of point mutants of PS2.M were synthesized, in which individual guanines were replaced by either hypoxanthine (I) or adenine (A). The sequences of the mutant oligonucleotides are given in Materials and Methods.

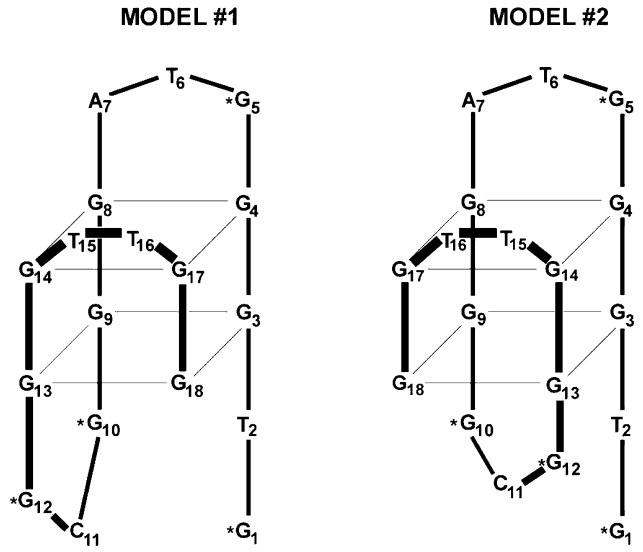

Fig. 2 Two related but topologically distinct models for the potassium-folded PS2.M. The guanines participating in quartet formation are the same set in the two models. The guanines indicated with asterisks are anticipated to be in the loops.

Methylation analysis of PS2.M point mutants

Methylation protection in both the presence and absence of hemin was carried out with each individual mutant oligonucleotide, and the results were analyzed as with PS2.M itself. Figure 3 shows the data for four characteristic mutants, G12A, G12I, G17A, and G18A. Neither the G17A nor the G18A oligonucleotide shows any evidence of methylation protection, in the presence or absence of hemin. Such a

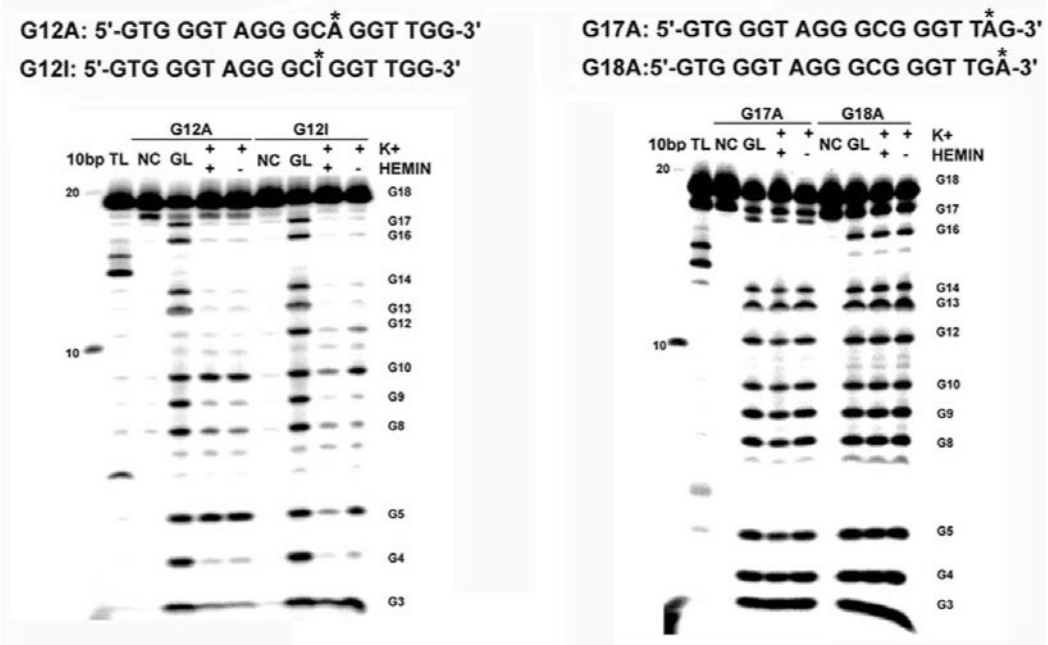

Fig. 3 Methylation protection gels for the point mutans G12A, G12I, G17A, and G18A. 'TL' shows thymine ladders for the relevant oligonucleotides; 'GL' shows guanine ladders.

result is consistent with our hypothesis that these point mutations are unable to support G-quadruplex folding in the manner shown in the models for the folded PS2.M (Fig. 2) in which both G17 and G18 participate in quartet formation. The G12I mutant, in both the presence and absence of hemin, substantially replicates the methylation patterns seen with PS2.M. With the G12A mutant, in the absence of hemin, essentially the methylation protection patterns of PS2.M are observed; however, the addition of hemin does not substantially change this pattern. Thus, a mutant with a G to I transition shows evidence of hemin binding; whereas a G to A transition abolishes such binding (or reduces the binding constant dramatically). G12 can thus be implicated in participating in hemin binding.

Table 1 summarizes the methylation data obtained from all of the mutant oligonucleotides. The partial methylation protection pattern characteristic of PS2.M in the absence of bound hemin is designated as '1', whereas the fuller protection in the presence of bound hemin is designated as '2'. The absence of any methylation protection, such as with G17A or G18A described above, is indicated as a '0'. Overall, it is possible to summarize that mutants G5A, G9A, G17A, and G18A appear not to form a quadruplex at all. This is consistent with G9, G17, and G18 all being presumptive quartet-forming guanines in the models shown in Fig. 2. The case of G5 is more interesting. G5A does not form a quadruplex either with or without hemin; however, G5I behaves normally, essentially like PS2.M. It is conceivable that a G to A mutation at this loop nucleotide generates an alternative, non-quadruplex folded structure for this oligonucleotide.

Table 1 A summary of data from various structure–function probing experiments carried out on PS2.M and on point mutants of PS2.M.

DNA	Peroxidase rate acceleration	T_m (°C)	Gel mobility	Methylation protection (– hemin)	Methylation protection (+ hemin)
PS2.M	5.4	52	+++	1	2
G1A	1.8	52	++++	N/A	N/A
G5A	1.0	36	+	0	0
G5I	1.3	42	++	1	2
G9A	1.0	–	+	0	0
G10A	0.9	48	++	0	1
G10I	1.2	51	++++	1	1
G12A	0.9	52	++++	1	1
G12I	1.5	48	+++	1	2
G17A	0.9	–	+	0	0
G18A	1.0	–	+	0	0
Hemin	1.0	N/A	N/A	N/A	N/A

The G1A mutant shows a methylation protection pattern, which in turn modifies when hemin is bound (data not shown), but both patterns are anomalous, i.e., different from those of PS2.M, and suggesting a different quadruplex formed by this oligonucleotide. As such, this is consistent with G1 being indeed extraneous to the quartets forming in folded PS2.M.

In both models shown in Fig. 2, G10 is a loop guanine located proximal to G12. As with G12, the G → I transition at this site is more permissive than the G → A transition. The G10 and G12 data cumulatively suggest that both guanines are likely proximal to a bound hemin, which one might hypothesize binds to PS2.M by π-stacking upon the terminal G-quartet formed by G3, G9, G13, and G18.

Native gel mobility analysis for mutant versions of PS2.M

An independent method for testing the formation of stably folded structures by the PS2.M mutants, relative to PS2.M itself, is by native gel electrophoresis. The gel mobilities of the different PS2.M mutants,

in the presence as well as absence of added hemin, were examined in native polyacrylamide gels run in TBE buffer supplemented with 5 mM KCl. Figure 4 shows typical data, for PS2.M and for the mutants G10A, G17A, and G18A. The complete results are summarized in Table 1. First, the mobility of each mutant oligonucleotide in the presence of hemin was found to be essentially identical to its mobility in the absence of hemin under our experimental conditions. This was likely due to dissociation of the hemin-DNA complex during the running of the gel rather than due to an intrinsic identity of gel mobility between the two. Overall, a number of mutants showed comparable or even higher mobility than PS2.M, whereas a few were notably slower than PS2.M. Those with comparable or faster mobility than PS2.M included G10I, G12A, and G12I, all of which also shared similar methylation protection patterns to PS2.M. By contrast, G5A, G9A, G17A, and G18A showed very slow gel mobilities, consistent with their not folding stably into a secondary structure, and consistent, too, with their overall lack of methylation protection. Overall, these gel mobility data correlated strongly with the methylation protection data (above) in suggesting the formation or lack of formation of stably folded G-quadruplex structures by the different mutants.

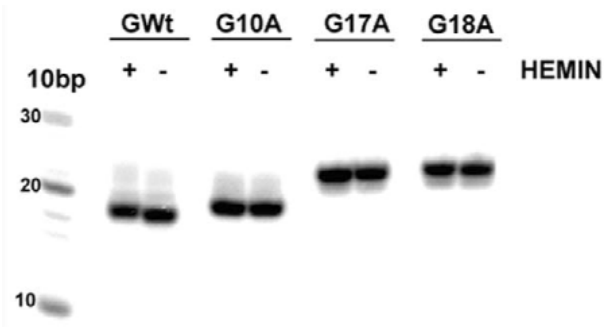

Fig. 4 Native gel mobility data for different PS2.M point mutants.

Melting behavior of folded PS2.M mutants

A third independent measure of the structural robustness of folded structures formed by the PS2.M and its mutants complexed with hemin was their thermal melting behavior. Melting was monitored at 295 nm, which has been shown to be the optimal wavelength for monitoring G-quadruplex-*specific* structural transitions [15]. Table 1 summarizes the melting point data for the PS2.M mutants. PS2.M itself had a T_m of 52 °C. Mutants G1A, G10A, G10I, G12A, and G12I had melting points equal to or close to 52 °C. By contrast, G5A and G5I had significantly lower melting points; whereas G9A, G17A, and G18A showed no melting transitions whatsoever, consistent with their not forming stably folded structures. Overall, as seen in Table 1, the melting data, too, were largely consistent with the methylation protection and the gel mobility data.

Peroxidase activity of folded PS2.M-hemin complexes

Finally, the ability of the various PS2.M mutants, when complexed with hemin (if indeed they were to able complex hemin), to catalyze the peroxidase reaction characteristic of PS2.M was investigated. Figure 5 shows the peroxidation rate vs. time profiles of disaggregated hemin alone; PS2.M-hemin; and the putative hemin complexes of the different PS2.M point mutants. It can be seen that PS2.M shows a superior activity relative to hemin alone as well as to all of the point mutants. The peroxidase rate acceleration afforded by each PS2.M mutant (relative to the rate from uncomplexed hemin) is summarized in Table 1. A number of the mutants showed activity no greater than hemin alone; this included mutants such as G5I and G12I, which from the other analyses described above, had very similar fold-

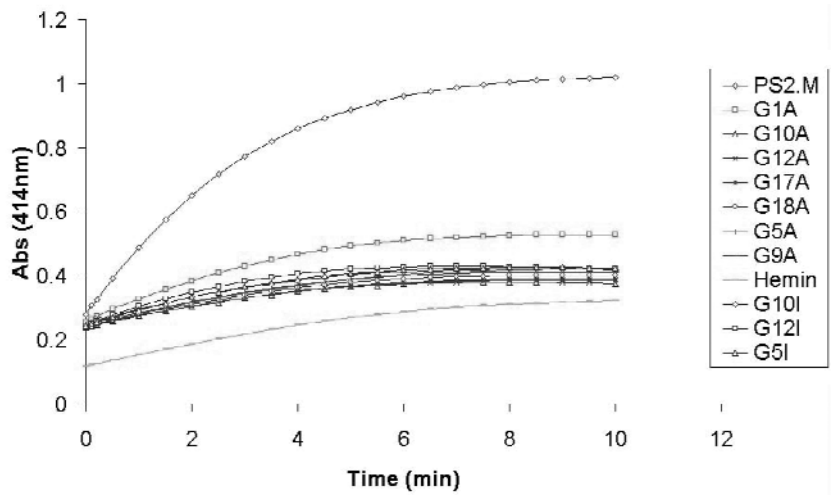

Fig. 5 Peroxidation rate (shown as ABTS radical absorbance) vs. time profiles for hemin; PS2.M-hemin, and hemin complexed to different PS2.M point mutants.

ing and hemin-binding properties as PS2.M itself. Nevertheless, the catalytic activity ($k_{observed}$) of PS2.M under these questions was >5-fold higher than the background (hemin alone) activity; whereas the best of the mutants, G1A, showed only <2-fold rate acceleration relative to the uncomplexed hemin background.

CONCLUSIONS

Methylation protection data were used to construct two closely related structural models for the folded PS2.M, which both contained two guanine quartets (involving the same guanines), but somewhat different loop topologies. On the basis of these folding models, a number of point mutants of PS2.M were generated and tested for their ability to fold comparably to PS2.M and also to catalyze peroxidation. Results obtained from thermal melting, gel mobility, as well as methylation protection data on the mutants were fully consistent with the structural models postulated for PS2.M. Guanines that were proposed in the models to be participating in quartet formation indeed could not be replaced with other purines. The roles of the guanines postulated to be in the loops of the quadruplex were more complex; significant differences in properties between G → A and G → I mutations implicated G10 and G12 as participatory in hemin binding and potentially in the catalysis of the peroxidase reaction.

A remarkable finding from the various experiments was that the "wild-type" PS2.M sequence was really the optimal one for the deoxyribozyme's peroxidase activity, and that even small and conservative changes, such as G → I transitions at the 5 and 12, which otherwise appeared to leave both the folding and heme-binding properties of the deoxyribozyme more or less intact, nevertheless showed far poorer catalytic activity than the original PS2.M sequence. Earlier data had established that an unrelated guanine quadruplex, OXY4, when complexed with hemin, was comparably poor at catalyzing peroxidation as the bulk of the PS2.M point mutations [11,12]. Current investigations (unpublished data) focus on the precise mechanism of catalysis of peroxidation by PS2.M and on the role(s) of specific nucleotides and functionalities within PS2.M on that catalysis.

ACKNOWLEDGMENTS

This work was funded by the Natural Sciences and Engineering Research Council of Canada. We thank the members of the Sen lab for suggestions and help. D.S. is a Senior Scholar of the Michael Smith Foundation for Health Research.

REFERENCES

1. K. Kruger, P. J. Grabowski, A. J. Zaug, J. Sands, D. E. Gottschling, T. R. Cech. *Cell* **31**, 147–157 (1982).
2. C. Guerrier-Takada, K. Gardiner, T. Marsh, N. Pace, S. Altman. *Cell* **35**, 849–857 (1983).
3. W. Gilbert. *Nature* **319**, 618 (1986).
4. A. D. Ellington and J. W. Szostak. *Nature* **346**, 818–822 (1990).
5. C. Tuerk and L. Gold. *Science* **249**, 505–510 (1990).
6. D. Sen and C. R. Geyer. *Curr. Opin. Chem. Biol.* **2**, 680–687 (1998).
7. Y. Li, C. R. Geyer, D. Sen. *Biochemistry* **35**, 6911–6922 (1996).
8. Y. Li and D. Sen. *Nat. Struct. Biol.* **3**, 743–747 (1996).
9. Y. Li and D. Sen. *Biochemistry* **36**, 5589–5599 (1997).
10. Y. Li and D. Sen. *Chem. Biol.* **5**, 1–12 (1998).
11. P. Travascio, Y. Li, D. Sen. *Chem. Biol.* **5**, 505–517 (1998).
12. P. Travascio, A. J. Bennet, D. Y. Wang, D. Sen. *Chem. Biol.* **6**, 779–787 (1999).
13. P. Travascio, P. K. Witting, A. G. Mauk, D. Sen. *J. Am. Chem. Soc.* **123**, 1337–1348 (2001).
14. K. Witting, P. Travascio, D. Sen, G. A. Mauk. *Inorg. Chem.* **40**, 5017–5023 (2001).
15. J. L. Mergny, A. T. Phan, L. Lacroix. *FEBS Lett.* **435**, 74–78 (1998).